"Physics of Auroral Phenomena", Proc. XXXVI Annual Seminar, Apatity, pp. 51 - 54, 2013

Polar Geophysical Institute

THE MAGNETOSPHERIC MAGNETIC FIELD DEFORMATION: EFFECTS OF DOUBLE-LOOP SUBSTORM CURRENT WEDGE

A.V. Nikolaev[1], V.A. Sergeev[1], N.A. Tsyganenko[1], V. Angelopoulos[2], H. Singer[3]

[1]*Saint-Petersburg State University, St.-Petersburg, Russia*
[2]*University of California, Los Angeles, USA*
[3]*Space Weather Prediction Center (NOAA), Boulder, USA*

Abstract. Recent studies of magnetic field dipolarization amplitudes simultaneously observed by one GOES and four THEMIS spacecraft radially-distributed in the magnetotail have confirmed a double-loop (R1-like plus R2-like) geometry of the Substorm Current Wedge (SCW) and introduce and test the new magnetospheric quantitative model SCW2L. To demonstrate and quantify the double-loop current system field line twisting effect we map fixed neutral sheet points to the ionosphere using T89 and SCW2L magnetic field models and show the possible shapes of active ionospheric structures (such as auroral bulge, westward traveling surge) which can appear when the substorm current system arise. Using quantitative SCW2L model and varying its parameters (current intensities, their ratio, field line stretching amplitude and currents intensity) we show that: (1) the poleward footprints expansion maximal amplitude may reach $\Delta Lat \sim 9^0$ CGLat during rare strong substorms (I_1 = 2 MA), $\Delta Lat \sim 5\text{-}6^0$ CGLat in moderate conditions (I_1 = 1 MA) and $\Delta Lat < 3^0$ during low level disturbances (I_1 < 0.5 MA); (2) the SCW-related magnetic disturbances can naturally explain the auroral bulge poleward expansion, westward traveling surge formation, auroral streamers morphology and their clockwise and westward/eastward movement. Our study is a continuation of earlier observational and theoretical studies devoted to the SCW morphology and its impact on the aurora displays and magnetospheric magnetic field configuration.

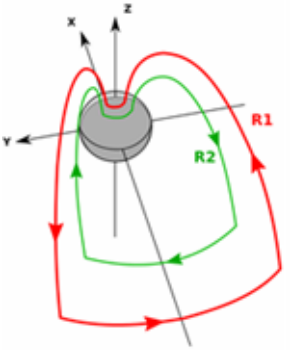

Fig. 1 The classic Substorm Current Wedge ("region 1" sense, red curve) and additional opposite polarity R2 current loop (green curve, "region 2" sense).

Introduction

The classical view on SCW (also referred to as the R1 loop) presented in Fig. 1 shows wedge-shaped structure (northern hemisphere) and its currents directions. The history of R1 loop models is long enough and we will not dwell on it noting that the recent realistic version of magnetospheric model (FW-SCW) detailed in *Sergeev et al.*, [2011] proved to be suitable for accurate magnetic field computations both in space and Earth's surface. However, geostationary magnetic observations compared with FW-SCW predictions systematically mismatched and indicated the need for additional "region 2" sense current loop also referred to as the R2 loop (see Fig. 1, green curve) to be added to traditional single-loop model. Previously using twin-loop SCW model version (SCW2L, presented in Fig. 1) and ground-based/spacecraft observations we estimated radial distance to R2 loop location (RT_2), current intensities and their ratio during real substorms expansion phase. Statistical studies of relationship between dipolarization amplitudes at 6.6 Re and 11 Re shown that magnetotail stretching amplitude (RCF parameter which is based on BZ_0 value at geostationary just prior to onset) corresponds to events of different intensities and associated R2 equatorial current locations. The strongly stretched configuration (RCF $\geq$ 6) allows earthward moving plasma injections, carrying dipolarization front (DF) and generating R2 wedge currents, penetrate closer to Earth ($RT_2 \leq$ 6.6 Re), while dipole-like configuration (RCF < 3) causes BBFs stop tailward the geostationary (RT_2 > 6.6 Re). In current study we apply SCW2L model to quantitatively investigate its magnetospheric effects and describe common auroral features appearing in azimuthal current wedge sector and at its edges.

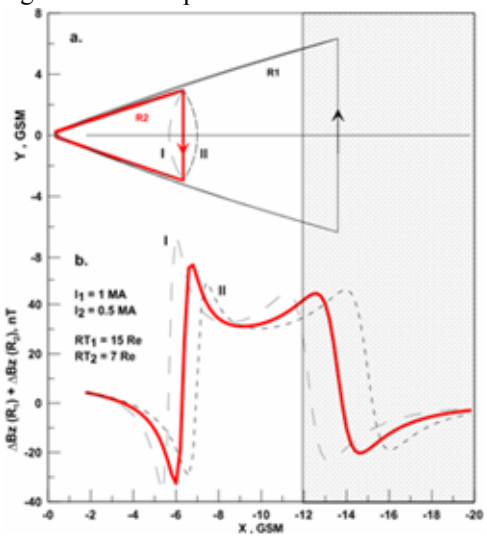

Fig. 2 View from the North: a) R2 (R1) loop location and configuration with concave (I) and convex (II) equatorial current segments; b) corresponding B_Z magnetic radial profiles calculated along X axis in XY plane (Y=0). The calculations performed for Pw = 155^0 SM Lon, Pe = 205 SM Lon.

SCW2L model setup

The SCW2L model is parameterized by total R1 and R2 currents (termed as I_1 and I_2), east and west SCW longitudes (Pe and Pw), and radial distances to equatorial location of R1 and R2-sense currents (RT_1 and RT_2, correspondingly). The shape of magnetic field lines, carrying SCW currents, is described by T89 model [*Tsyganenko*,

1989] and its background magnetic field stretching parameter (RCF).To neglect the asymmetry of SCW with respect to neutral sheet and midnight meridian, we fix FACs central longitude at midnight and perform calculations on 2009/09/05 at 08:00:00 UT, when the dipole tilt angle value was ~0. In addition, the transverse current spread (D_0), scaled as $D^2 \sim R^{3/2}$, was not allowed to exceed 2 Re at tailward distances greater than R = 8 Re, where its half-thickness D was equal to 0.5 Re. The RT_1 is fixed at 15 Re. In addition we require both current loops span the same longitudinal sector (i.e. Pw and Pe values equal for both wedges).Taking into account a complicate topology of R2 duskward current, we reproduce its extreme shapes (see Fig. 2a) as concave and convex contours I and II and calculate magnetic radial profiles along X axis (Y=0) for three different SCW2L configurations (Fig. 2b, I, II and red solid curves). The total current intensities was set in this example to be I_1 = 1 MA and I_2 = 0.5 MA, while Pw and Pe for both loops was kept fixed at 155^0 and 205^0 SM Lon, correspondingly. As seen from Fig. 2b, difference between magnetic radial profiles of I and II curves is significant, so we remove its curvature and use simple straight-line connection between FACs (red wedge at Fig. 2a). Red solid line plotted at Fig. 2b shows magnetic field disturbance generated by R1 plus R2 currents.

Ionospheric footprint displacement due to SCW

Choosing points of the neutral sheet as starting locations in the night side magnetosphere, we trace magnetic field lines to ionospheric heights (R = 1.02 Re) two times: first time we use standard T89 model [*Tsyganenko*, 1989] and second time, combination of T89 and SCW2L models. The latitudinal and longitudinal difference between corresponding neutral sheet footprints is measured by geocentric angle expressed as

$$\alpha = \arccos\left(\frac{X_1 X_2 + Y_1 Y_2 + Z_1 Z_2}{R^2}\right)$$

where R = 1.02 Re, and [X, Y, Z] is the footprint coordinates [GSM] obtained by two trace procedures. Fig. 3 graphically illustrates (1) amplitudes of mapping distortions (by color), (2) R1 and R2 loop configurations in XY plane and (3) radial distance to R2 cross-tail current (RT_2 = 6 Re). Corresponding current intensities are I_1 = 1 MA and I_2 = 0.5 MA, which can be met during strong and rather rare substorms.

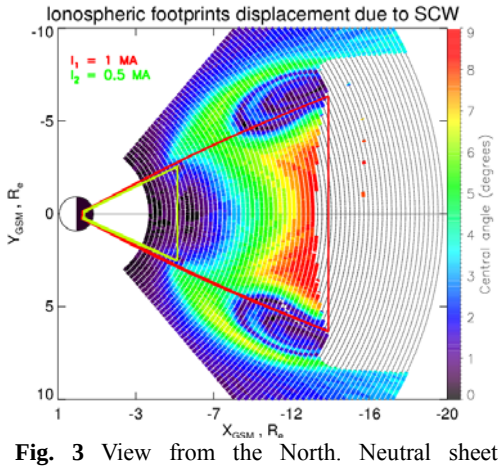

Fig. 3 View from the North. Neutral sheet locations traced to ionosphere with addition of the substorm current wedge magnetic field. Color indicates amplitudes of ionospheric footprints deformation after adding SCW2L model in terms of geocentric angle. Location of R1 and R2 loops are also presented. The calculations performed for Pw = 155^0 SM Lon, Pe = 205^0 SM Lon., RT_1 = 15 Re, RT_2 = 6 Re.

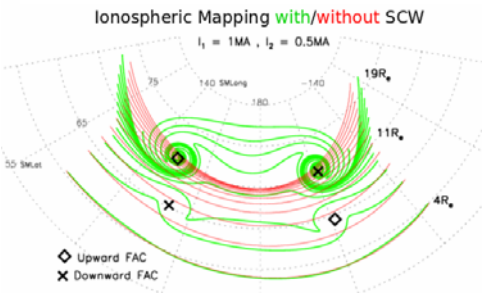

Fig. 4 Ionospheric pattern of the equidistant neutral sheet lines projections obtained without (red) and with (green) addition of the Substorm Current Wedge magnetic effects.

In order to visualize ionospheric footprint shifts, colored in Fig. 3, we map the set of equidistant neutral sheet points (drawn at Fig. 3 as azimuthal arcs) to nightside ionospheric plane and illustrate it on Fig. 4. Red lines indicate arcs (with radius of curvature covering range of distances from R = 4 Re to R = 20 Re) traced with IGRF plus T89 models, while the green ones show the same arcs, mapped with addition of SCW2L model. The square and cross symbols correspond to upward and downward FACs footprints.

Red and green contours together with Fig. 3 graphically illustrate the pattern of ionospheric distortions, consisting of three specific areas. The first one is the region, localized between equatorial R1 and R2 currents inside SCW azimuthal sector, where footprints poleward shift reach its maximum value when approaching the R1 loop currents (red area at Fig. 3). The second ones form a rotational type of displacement in the region, where the magnetic field lines explicitly twisted by the FACs. The R2 field-aligned currents have a smaller contribution to the mapping distortion, because they act in the region of strong background magnetic field and their intensity is lower than that, flowing in R1 loop. The third black doted area at Fig. 3 corresponds to the region of weak magnetotail field, strongly disturbed by the magnetic field of R1 equatorial current. The O-type field lines appear at those locations and prevent connection between ionosphere and plasma sheet, so we excluded that region from analysis. In addition, vortices centered at the points of FACs projections are not analyzed because the small-scale SCW signatures cannot be described by highly idealized SCW2L model, which is only suitable for the diagnostics of large-scale magnetic field changes.

Footprint displacement depending on SCW parameters

Current intensities play an important role in substorm-time magnetospheric diagnostics, because R1 and R2 wedges can both enhance and compensate for each other magnetic effects in different observational locations. The ground-based magnetometer

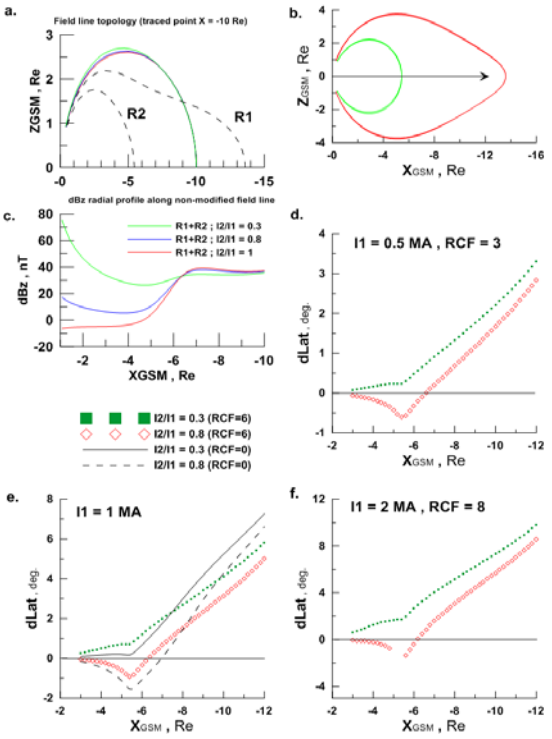

Fig. 5 Footprints shifts for the points lying in the X axis (Y=0) in the XY plane: a) XZ cut of the SCW FACs and the shape of field lines starting from X = -10 Re; c) B_Z magnetic radial profile obtained from SCW2L along field lines at a) plot; d) latitudinal shifts for moderate substorms (I_1 = 0.5 MA) for I_1/I_2 = 0.3 and 0.8; e) latitudinal shifts for stronger events for two values of I_1/I_2 and RCF; f) the same as in d) but for I_1 = 2 MA, RCF = 8.

inside the azimuthal sector of two wedges of opposite polarities observes bay-like variations, characterized by I_1-I_2, while spacecraft located in between R1/R2 loops registers cumulative current effects I_1+I_2. The intense currents obviously lead to the greatest magnetic field changes (according to Biot-Savart law), particularly in the area lying between wedges (red colored region at Fig. 3) where the effects of R1 and R2 current loops are added. Our study focuses on the contribution of SCW2L parameters (such as I_1, RCF and I_2/I_1) to mapping distortions, so we fixed RT_2 = 6 Re in the region of strong background magnetic field and examined the latitudinal footprints shift (plotted at Fig. 5d-f) for the set of equatorial points (Fig. 5b) lying in the center of SCW azimuthal sector (Y=0, Z=0).

Calculations performed for moderate (I_1 = 0.5 MA, Fig. 5d), strong (I_1 = 1 MA, Fig. 5e) and extremely strong (I_1 = 2 MA, Fig. 5f) substorms showed that the poleward footprints expansion rather small in first case (~ 2-3^0 CGLat), increases in the second case (~ 5 – 6^0 CGLat) and maximizes in third case (~ 9^0 CGLat). The enhanced R2 current ($I_2/I_1 \geq 0.5$) decreases the amplitude of maximal latitudinal displacement by < 20% and causes small equatorward footprint shift in vicinity of R2 current latitudes. This effects are explained by Fig. 5c illustrating the B_Z magnetic profile built with SCW2L model (I_1 = 1 MA) along the T89 model field line starting from X = -10 Re [GSM]: in vicinity of equatorial plane magnetic field is enhanced by SCW-related depolarization (ΔB_Z>0), but in tail lobes it is depressed by nearby R2 FACs (ΔB_Z< 0), thus magnetic field lines is deformed as shown in Fig. 5a. The red curve gap which is visible in Fig. 5f is the region, where the strong R2 equatorial current (I_2 = 1 MA) forms the loop magnetic field line and prevent connection between ionosphere and plasma sheet. As for the background magnetic field stretching parameter (RCF), it slightly varies the footprints ΔLat by ~ 1-2^0 CGLat as seen from Fig. 5e, where black lines go higher than colored ones.

Relationship between SCW and auroral streamers

From a wide range of auroral manifestation during substorm expansion phase we can distinguish North-South auroral forms (NS) emerging within auroral bulge. *Henderson et al.,* [1994] schematically illustrated the occurrence of north-south auroral forms in the active poleward region of auroral bulge (termed as "traversing arc") in vicinity of the surge head. Authors showed that some of NS are ejected from the intensifying traversing arc, drift equatorward, then split and continue its propagation westward/eastward (see Fig. 9.2 in *Henderson et al.,* 1994) with the tendency to rotate clockwise in the region lying nearby WTS. Results obtained from spacecraft observations have been supported by *Nakamura et al.,* [1993] who compiled ground-based optical observations of eight all-sky TV cameras and illustrated similar dynamics of the poleward boundary and NS. The conjunction of auroral streamers with the earthward moving transient bursty bulk flows (BBFs) was discussed in e.g. *Nakamura et al.,* [2001], *Henderson et al.,* [2012], *Lyons et al.,* [2012]. Concentrated current leaving the ionosphere generates vortex-like magnetic field, which twist nearby field lines and causes their footprints rotate around location of FACs.

To illustrate it we mapped to the ionosphere the neutral sheet locations presented in Fig. 6a as narrow radially-aligned structures morphologically similar to BBFs (in "zero" approximation). The color changes in the direction of BBF movement along straight trajectories in plasma sheet. Black north-south aligned strips in Fig. 6b reflects ionospheric BBFs paths calculated with IGRF plus T89 model, while colored ones reflect corresponding trajectories obtained by addition of SCW2L model with I_1 = 1 MA, I_2 = 0.5 MA, RT_2=6 Re and RCF=6. Predicted NS auroral forms are divided into two groups: first one, reflects BBFs moving in the FAC vicinity where magnetic field configuration is highly sensitive to enhanced SCW-related By-magnetic component responsible for the twist of the magnetic field line; in the second group neutral sheet locations in a central SCW longitude are traced along field lines disturbed by strong positive B_Z magnetic component, which shifts ionospheric footprints poleward.

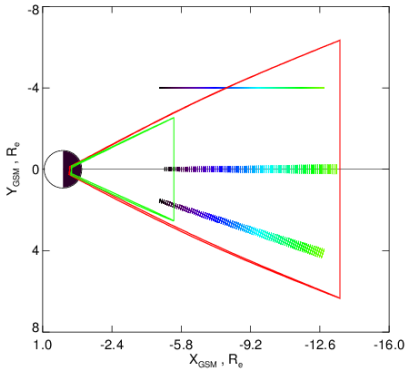

Fig. 6a View from North. R1 and R2 loop locations in XY plane. Colored strips indicate traced structures similar in morphology with BBFs.

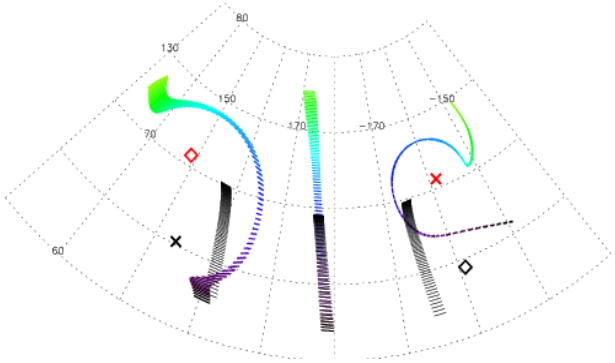

Fig. 6b Ionospheric projections of the strips drawn in fig. 6a obtained with (colored lines) and without (black lines) addition of SCW2L model. Model parameters are similar to those presented in fig. 3.

Conclusions

We quantitatively described the magnetospheric magnetic field deformations for the set of basic SCW2L parameters in a simple symmetric geometry. The substorm current wedge two-loop configuration and its parameters approach does not provide complete information about auroral structures or about magnetospheric field distortions during real magnetospheric substorm, but gives an idea of the amplitudes of ionospheric footprints displacement for different activity levels and predicts common forms of active aurora. We found, that the R1 loop intensity is the most effective parameter, which strongly contributes ionospheric footprints shifts. The latitudinal displacement may reach $\Delta Lat \sim 9^0$ CGLat during rare and strong substorms, do not exceed $\Delta Lat \sim 5\text{-}6^0$ CGLat in moderate and minimizes $\Delta Lat < 3^0$CGLat during low-level disturbances. This estimations are consistent with earlier predictions by *Vasilyev et al.*, [1986], who showed that amplitude of auroral bulge expansion for current intensities $I_1 = 1$ MA approximately 7^0 CGLat. In terms of SCW2L model difference in two degrees can be explained by R2 loop which depress dipolarization attributed to R1 loop. As for magnetic effects related to R2 loop, they slightly change ionospheric positions of neutral sheet points located in vicinity of R2 equatorial current, this change do not exceed $\Delta Lat \sim 2^0$ CGLat in equatorward direction. The neutral sheet footprints, changing their ionospheric locations due to SCW, forms auroral bulge structure. This effect was first noticed by *Vasilev et al.,* [1986] on a basis of a simple wire-like SCW model. Moreover, helical magnetic field existing near FACs leads to a twisting of magnetic field lines as a result, appearing WTS bends at the dusk and dawn side boundaries of the auroral bulge. Such ionospheric pattern caused by magnetic field reconfiguration can be used as a natural explanation of substorm manifestation in high-latitude active aurora.

References

Henderson, M. G. (2012) Auroral Substorms, Poleward Boundary Activations, Auroral Streamers, Omega Bands, and Onset Precursor Activity, in Auroral Phenomenology and Magnetospheric Processes: Earth And Other Planets (eds A. Keiling, E. Donovan, F. Bagenal and T. Karlsson), American Geophysical Union, Washington, D. C. doi: 10.1029/2011GM001165.

Henderson, M. G., J. S. Murphree, G. D. Reeves (1994), The activation of the dusk-side and the formation of north-south aligned structures during substorms, in proceedings of the Second international Conference on substorms (ISC-2), edited by J. R. Kan, J. D. Craven, S. Akasofu, p. 37, Geophys. Inst., Univ. Alaska, Fairbanks.

Lyons, L. R., Nishimura, Y., Xing, X., Shi, Y., Gkioulidou, M., Wang, C.-P., Kim, H.-J., Zou, S., Angelopoulos, V. and Donovan, E. (2012) Auroral Disturbances as a Manifestation of Interplay Between Large-Scale and Mesoscale Structure of Magnetosphere-Ionosphere Electrodynamical Coupling, in Auroral Phenomenology and Magnetospheric Processes: Earth And Other Planets (eds A. Keiling, E. Donovan, F. Bagenal and T. Karlsson), American Geophysical Union, Washington, D. C.. doi: 10.1029/2011GM001152.

Nakamura, R., T. Oguti, T. Yamamoto, S. Kokubun (1993), Equatorward and poleward expansion of the auroras during auroral substorms, J. Geophys. Res., 98(A4), 5743-5759.

Sergeev, V. A., L. I. Vagina, R. D. Elphinstone, J. S. Murphee, D. J. Hearn, M. L. Johnson (1996), Comparison of UV optical signatures with the substorm current wedge predicted by an inversion algorithm, J. Geophys. Res., 101, P. 2615-2627.

Sergeev, V. A., N. A. Tsyganenko, M. V. Smirnov, A. V. Nikolaev, H. J. Singer, and W. Baumjohann (2011), Magnetic effects of the substorm current wedge in a 'spread-out wire' model and their comparison with ground, geosynchronous, and tail lobe data, J. Geophys. Res., 116, A07218, doi:10.1029/2011JA016471.

Tsyganenko, N.A. (1989), A magnetospheric magnetic field model with warped tail current sheet, Planet. Space Sci., 37, 5-20.

Vasilyev, E. P., M. V. Malkov, V. A. Sergeev (1986), Three-dimensional effects of Birkeland's current loop, Geomagn. And Aeronomy, V. 26, P. 114, №1.